

## Rate equations for the study of femtosecond intervalley scattering in compound semiconductors

C. J. Stanton

*Department of Physics, University of Florida, Gainesville, Florida 32611*

D. W. Bailey

*Department of Electrical and Computer Engineering, University of South Carolina, Columbia, South Carolina 29208*

(Received 30 September 1991; revised manuscript received 9 December 1991)

We present solutions to a set of rate equations for the electron dynamics after photoexcitation by a 2.0-eV laser in GaAs and InP. Results obtained, although simpler than full Monte Carlo solutions, closely follow the experimental data and provide insight into intervalley scattering. Calculations show that the net return time of electrons from the satellite  $L$  valleys into the  $\Gamma$  valley is not limited by the intervalley scattering rate, but is instead limited by the polar-optic-phonon scattering rate within the  $\Gamma$  valley. This shows that the time-dependent mobility and luminescence experiments depend on the  $L$ -valley depopulation rate, which differs from the  $L \rightarrow \Gamma$  intervalley scattering rate. Results further suggest that the  $\Gamma \rightarrow L$  scattering rate is faster than the polar-optic-phonon scattering rate.

### INTRODUCTION

Intervalley scattering in compound semiconductors is responsible for the transferred electron effect<sup>1</sup> and is thus important in the operation of Gunn oscillators and microwave devices. As a result, there is interest in accurately measuring the intervalley scattering rates. With the development of ultrafast lasers, experiments with a time resolution comparable to the intervalley scattering times have become possible. These experiments include the rise time of band-edge photoluminescence,<sup>2,3</sup> pump-infrared-probe absorption,<sup>4</sup> femtosecond reflectivity,<sup>5</sup> equal pulse correlation,<sup>6,7</sup> pump-continuum-probe absorption,<sup>8</sup> transient nonlinear absorption,<sup>9,10</sup> and cw acceptor luminescence.<sup>11-13</sup>

Several of these experiments claim to measure the deformation potential phonon scattering rate in GaAs for the scattering of carriers from the satellite  $L$  valleys back into the central  $\Gamma$  valley. The values reported for the deformation potential constant  $D_{\Gamma L}$ , however, have a large variance.<sup>13</sup> In this paper, we show, through a series of rate-equation models, that the time measured in some of these experiments is *not* the  $L \rightarrow \Gamma$  scattering rate, but the  $L$ -valley depopulation rate. This suggests that the apparent controversy is due in part to a misinterpretation of some of the experiments.

Comparison of our calculations to luminescence and mobility experiments shows that in GaAs, the  $L$ -valley depopulation rate is most strongly influenced by the rate of inelastic scattering, chiefly the polar-optic-phonon (POP) emission rate, *within* the  $\Gamma$  valley. If the inelastic scattering rate in the  $\Gamma$  valley is small compared to the  $\Gamma \rightarrow L$  scattering rate, then to lowest order, the  $L$ -valley depopulation rate *does not depend* on the  $L \rightarrow \Gamma$  rate. For this case, the bottleneck for the return of electrons from the satellite  $L$  valleys to the central  $\Gamma$  valley is the cooling of the electrons in the  $\Gamma$  valley. The cooling of electrons allows a net flow of electrons from the  $L$  valley

into the  $\Gamma$  valley. In addition, our studies show that the  $\Gamma \rightarrow L$  scattering rate is larger than the POP scattering rate.

This paper is organized as follows. We start with a two-state rate-equation model. While this model is too simple to describe optical experiments in GaAs, it illustrates an important point, namely that the two intervalley scattering rates  $\Gamma \rightarrow L$  and  $L \rightarrow \Gamma$  are *not independent* but are related through the density of states in each valley. We then extend our method to a three-state model. This allows us to describe actual experiments in GaAs provided that the measured quantities depend only on the valley the electrons occupy and not on the details of the electron states within each valley. (An example of such an experiment is the femtosecond mobility experiments of Nuss, Auston, and Capasso.<sup>5</sup>) Finally, we extend the three-state model to a four-state model. With four states, we can account for experiments that are sensitive not only to which valley the electrons occupy, but also are sensitive to which state within the valley the electron occupies. For example, in the time-resolved luminescence experiments of Shah *et al.*,<sup>2</sup> only electrons at the bottom of the conduction band contribute to the luminescence signal.

### TWO-STATE MODEL

We start with a two-state model shown in Fig. 1. It is the simplest possible model, but illustrates several key points about electron relaxation in compound semiconductors. One state represents all electrons in the  $\Gamma$  valley and the other represents all electrons that are in the  $L$  valleys.  $\gamma_{\Gamma L}$  is the  $\Gamma \rightarrow L$  scattering rate, and  $\gamma_{L\Gamma}$  is the  $L \rightarrow \Gamma$  scattering rate.

This is not a realistic model for carrier dynamics in compound semiconductors because it does not allow for states in the  $\Gamma$  valley that are not energetically able to scatter into the  $L$  valley. That is, relaxation of electrons

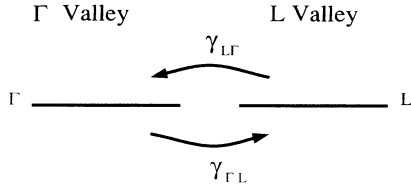


FIG. 1. The two-state model for intervalley scattering in compound semiconductors. The state  $\Gamma$  represents all electrons in the central  $\Gamma$  valley, while the state  $L$  represents all electrons in the  $L$  valleys. No distinction is made between electrons within a given valley.  $\gamma_{\Gamma L}$  is the  $\Gamma$  to  $L$  scattering rate and  $\gamma_{L\Gamma}$  is the  $L$  to  $\Gamma$  scattering rate.

in the  $\Gamma$  valley is ignored. Nonetheless, this model is instructive for the analysis of more complex systems and has features applicable to real systems.

The rate equations in this model are given in matrix form by

$$\frac{d}{dt} \begin{pmatrix} n_{\Gamma} \\ n_L \end{pmatrix} = \begin{pmatrix} -\gamma_{\Gamma L} & \gamma_{L\Gamma} \\ \gamma_{\Gamma L} & -\gamma_{L\Gamma} \end{pmatrix} \begin{pmatrix} n_{\Gamma} \\ n_L \end{pmatrix}. \quad (1)$$

Here  $n_{\Gamma}$  and  $n_L$  are the densities of electrons in the  $\Gamma$  and  $L$  valleys, respectively. A straightforward calculation shows that the eigenvalues and (unnormalized) eigenvectors are given by

$$\lambda_1 = 0, \quad \lambda_2 = -(\gamma_{\Gamma L} + \gamma_{L\Gamma}), \quad (2)$$

$$\mathbf{V}_1 = \begin{pmatrix} \gamma_{L\Gamma} \\ \gamma_{\Gamma L} \end{pmatrix}, \quad \mathbf{V}_2 = \begin{pmatrix} 1 \\ -1 \end{pmatrix}.$$

The zero eigenvalue results from the total density  $n_{\Gamma} + n_L$  being constant. The general solution to the two-state model is obtained by taking a superposition of the two eigensolutions:

$$\begin{pmatrix} n_{\Gamma}(t) \\ n_L(t) \end{pmatrix} = A \begin{pmatrix} \gamma_{\Gamma L} \\ \gamma_{L\Gamma} \end{pmatrix} + B \begin{pmatrix} 1 \\ -1 \end{pmatrix} e^{-(\gamma_{\Gamma L} + \gamma_{L\Gamma})t}. \quad (3)$$

The constants  $A$  and  $B$  are determined by the initial conditions:

$$\begin{pmatrix} \gamma_{L\Gamma} & 1 \\ \gamma_{\Gamma L} & -1 \end{pmatrix} \begin{pmatrix} A \\ B \end{pmatrix} = \begin{pmatrix} n_{\Gamma}^0 \\ n_L^0 \end{pmatrix}. \quad (4)$$

Here  $n_{\Gamma}^0$  and  $n_L^0$  are the initial populations of carriers in the two valleys. Solving Eq. (4) for  $A$  and  $B$ , we obtain the solution

$$n_{\Gamma}(t) = \frac{n\gamma_{L\Gamma}}{\gamma_{\Gamma L} + \gamma_{L\Gamma}} + \left[ \frac{n_{\Gamma}^0\gamma_{\Gamma L} - n_L^0\gamma_{L\Gamma}}{\gamma_{\Gamma L} + \gamma_{L\Gamma}} \right] e^{-(\gamma_{\Gamma L} + \gamma_{L\Gamma})t}, \quad (5)$$

$$n_L(t) = \frac{n\gamma_{\Gamma L}}{\gamma_{\Gamma L} + \gamma_{L\Gamma}} - \left[ \frac{n_{\Gamma}^0\gamma_{\Gamma L} - n_L^0\gamma_{L\Gamma}}{\gamma_{\Gamma L} + \gamma_{L\Gamma}} \right] e^{-(\gamma_{\Gamma L} + \gamma_{L\Gamma})t}.$$

The total number of carriers  $n = n_{\Gamma}(t) + n_L(t) = n_{\Gamma}^0 + n_L^0$  is independent of time.

In equilibrium ( $t \rightarrow \infty$ ) the number of carriers in each

valley is found to be

$$n_{\Gamma}^{\text{eq}} = n_{\Gamma}(t \rightarrow \infty) = \frac{n\gamma_{L\Gamma}}{\gamma_{\Gamma L} + \gamma_{L\Gamma}}, \quad (6)$$

$$n_L^{\text{eq}} = n_L(t \rightarrow \infty) = \frac{n\gamma_{\Gamma L}}{\gamma_{\Gamma L} + \gamma_{L\Gamma}}.$$

From this, one obtains a ‘‘detailed balance’’ relation

$$\frac{\gamma_{L\Gamma}}{\gamma_{\Gamma L}} = \frac{n_{\Gamma}^{\text{eq}}}{n_L^{\text{eq}}} \equiv R. \quad (7)$$

$R$  is defined to be the equilibrium ratio of the populations in the two valleys. If a more detailed model based on a complete description of all states were considered, then intervalley scattering events would obey a detailed balance relation given by

$$W_{\Gamma \rightarrow L}^{k, k'} f_{\Gamma}^{\text{eq}}(\mathbf{k}) = W_{L \rightarrow \Gamma}^{k', k} f_L^{\text{eq}}(\mathbf{k}'), \quad (8)$$

with  $W_{\Gamma \rightarrow L}^{k, k'}$  the transition probability per unit time from state  $\mathbf{k}$  in the  $\Gamma$  valley to state  $\mathbf{k}'$  in the  $L$  valley.<sup>14</sup> This means that the  $\Gamma \rightarrow L$  and  $L \rightarrow \Gamma$  rates are *dependent*. Knowledge of one implies knowledge of the other.

Another point to note is that deviations from the equilibrium populations relax with a rate given by the *sum* of the two scattering rates  $\gamma_{\Gamma L} + \gamma_{L\Gamma}$ . That is, if  $\delta n_{\Gamma}(t) \equiv n_{\Gamma}(t) - n_{\Gamma}^{\text{eq}}$ , then

$$\delta n_{\Gamma}(t) = \left[ \frac{n_{\Gamma}^0\gamma_{\Gamma L} - n_L^0\gamma_{L\Gamma}}{\gamma_{\Gamma L} + \gamma_{L\Gamma}} \right] e^{-(\gamma_{\Gamma L} + \gamma_{L\Gamma})t}, \quad (9)$$

$$\delta n_L(t) = -\delta n_{\Gamma}(t) = \left[ \frac{n_L^0\gamma_{L\Gamma} - n_{\Gamma}^0\gamma_{\Gamma L}}{\gamma_{\Gamma L} + \gamma_{L\Gamma}} \right] e^{-(\gamma_{\Gamma L} + \gamma_{L\Gamma})t}.$$

This counters the naive assumption that a deviation from the equilibrium population in the  $\Gamma$  valley relaxes with  $\gamma_{\Gamma L}$  and a deviation in the  $L$  valley relaxes with  $\gamma_{L\Gamma}$ . Any deviation from the equilibrium ratio of carriers will relax with the combined rate  $\gamma_{\Gamma L} + \gamma_{L\Gamma}$ . While this seems strange for electrons in the  $L$  valley where the  $L \rightarrow \Gamma$  scattering rate is slower than the  $\Gamma \rightarrow L$  rate, it is important to remember that fewer electrons have to transfer from the  $L$  valley to restore the equilibrium ratio. Equation (9) means that the carrier densities in the two valleys equilibrate on a time scale comparable to the fastest of the two scattering times.

### THREE-STATE MODEL

The two-state model is simplistic since it does not consider that the  $\Gamma$  valley is made up of several states. In particular, there is an energy threshold within the  $\Gamma$  valley below which electrons can no longer scatter into the satellite  $L$  valleys. A more realistic model for intervalley transfer must allow for this. Such a model is given by the three-state model shown in Fig. 2. In the three-state model, states in the  $\Gamma$  valley are separated above and below  $\Delta$ , the energy threshold for transfer into the  $L$  valley. All  $\Gamma$  valley electrons with enough energy to transfer into the  $L$  valleys are in the  $\Gamma^>$  state; all  $\Gamma$  valley electrons with energy less than  $\Delta$  are in the  $\Gamma^<$  state; and

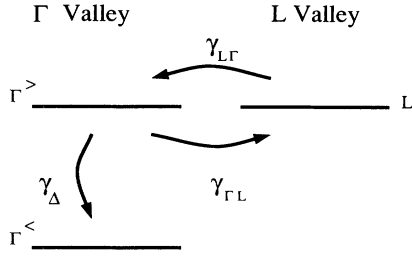


FIG. 2. The three-state model for intervalley scattering.  $\Gamma^>$  is the state that represents all electrons in the  $\Gamma$  valley which are energetically able to transfer into the  $L$  valley state. The  $\Gamma^<$  state represents all electrons in the  $\Gamma$  valley that do not have enough energy to transfer to the  $L$  valley state. Scattering from the  $\Gamma^>$  state to the  $\Gamma^<$  state occurs via inelastic scattering within the  $\Gamma$  valley with a rate  $\gamma_\Delta$ . This occurs mostly by POP emission.

electrons in the  $L$  valley are in the third state. Only electrons in state  $\Gamma^>$  can scatter into the  $L$ -valley state and electrons in the  $L$ -valley state can only scatter into the  $\Gamma^>$  state. Scattering from the  $\Gamma^>$  state into the  $\Gamma^<$  state is given by the scattering rate  $\gamma_\Delta$  and occurs through inelastic scattering within the  $\Gamma$  valley. This is chiefly through POP emission.<sup>15</sup> While POP absorption makes scattering from below  $\Delta$  to above  $\Delta$  possible, for simplicity it is ignored in this model because POP emission occurs more frequently.

Note that for simplicity we have not included scattering into the satellite  $X$  valleys. For 2.0-eV photoexcitation experiments, only a small fraction of the photoexcited electrons are energetically able to scatter into the  $X$  valleys so that this is a minor correction. For higher energies, the  $X$  valleys must be included, or the satellite valley state (and hence the appropriate scattering rates) modified to include both  $L$  and  $X$  valleys. Inclusion of an  $X$  valley should be straightforward.

The equations for the three-state model are given by

$$\frac{d}{dt} \begin{pmatrix} n_{\Gamma^>}(t) \\ n_L(t) \\ n_{\Gamma^<}(t) \end{pmatrix} = \begin{pmatrix} -(\gamma_{\Gamma L} + \gamma_\Delta) & \gamma_{L\Gamma} & 0 \\ \gamma_{\Gamma L} & -\gamma_{L\Gamma} & 0 \\ \gamma_\Delta & 0 & 0 \end{pmatrix} \begin{pmatrix} n_{\Gamma^>}(t) \\ n_L(t) \\ n_{\Gamma^<}(t) \end{pmatrix}. \quad (10)$$

The eigenvalues are

$$\lambda_0 = 0,$$

$$\lambda_\pm = -\frac{1}{2} \left[ (\gamma_{\Gamma L} + \gamma_{L\Gamma} + \gamma_\Delta) \pm \sqrt{(\gamma_{\Gamma L} + \gamma_{L\Gamma} + \gamma_\Delta)^2 - 4\gamma_{L\Gamma}\gamma_\Delta} \right]. \quad (11)$$

The unnormalized eigenvectors for the matrix in the three state model are given by

$$\begin{aligned} \mathbf{V}_0 &= \begin{pmatrix} 0 \\ 0 \\ \gamma_\Delta \end{pmatrix}, \\ \mathbf{V}_+ &= \begin{pmatrix} \lambda_+ \\ \frac{\gamma_{\Gamma L}\lambda_+}{\gamma_{L\Gamma} + \lambda_+} \\ \gamma_\Delta \end{pmatrix}, \\ \mathbf{V}_- &= \begin{pmatrix} \lambda_- \\ \frac{\gamma_{\Gamma L}\lambda_-}{\gamma_{L\Gamma} + \lambda_-} \\ \gamma_\Delta \end{pmatrix}. \end{aligned} \quad (12)$$

The general solution is

$$\begin{pmatrix} n_{\Gamma^>}(t) \\ n_L(t) \\ n_{\Gamma^<}(t) \end{pmatrix} = A\mathbf{V}_0 + B\mathbf{V}_+ e^{\lambda_+ t} + C\mathbf{V}_- e^{\lambda_- t}, \quad (13)$$

with  $A$ ,  $B$ , and  $C$  determined by the initial conditions

$$\begin{pmatrix} 0 & \lambda_+ & \lambda_- \\ 0 & \frac{\gamma_{\Gamma L}\lambda_+}{\gamma_{L\Gamma} + \lambda_+} & \frac{\gamma_{\Gamma L}\lambda_-}{\gamma_{L\Gamma} + \lambda_-} \\ \gamma_\Delta & \gamma_\Delta & \gamma_\Delta \end{pmatrix} \begin{pmatrix} A \\ B \\ C \end{pmatrix} = \begin{pmatrix} n_{\Gamma^>}^0 \\ n_L^0 \\ n_{\Gamma^<}^0 \end{pmatrix}. \quad (14)$$

Solving for  $A$ ,  $B$ , and  $C$  and using the relations

$$\begin{aligned} \lambda_+ \lambda_- &= \gamma_{L\Gamma} \gamma_\Delta, \\ (\gamma_{L\Gamma} + \lambda_+) (\gamma_{L\Gamma} + \lambda_-) &= -\gamma_{\Gamma L} \gamma_{L\Gamma}, \end{aligned} \quad (15)$$

we can find the final solution for the populations of the three states. For the experiments we are considering,<sup>2,5</sup> electrons are initially excited only into the  $\Gamma^>$  state, i.e.,  $n_{\Gamma^>}^0 \neq 0$ ,  $n_L^0 = 0$ ,  $n_{\Gamma^<}^0 = 0$ ; then

$$\begin{aligned} n_{\Gamma^>}(t) &= n_{\Gamma^>}^0 \left[ \left( \frac{\gamma_{L\Gamma} + \lambda_+}{\lambda_+ - \lambda_-} \right) e^{\lambda_+ t} - \left( \frac{\gamma_{L\Gamma} + \lambda_-}{\lambda_+ - \lambda_-} \right) e^{\lambda_- t} \right], \\ n_L(t) &= n_{\Gamma^>}^0 \left[ \left( \frac{\gamma_{\Gamma L}}{\lambda_+ - \lambda_-} \right) (e^{\lambda_+ t} - e^{\lambda_- t}) \right], \\ n_{\Gamma^<}(t) &= \frac{n_{\Gamma^>}^0 \gamma_\Delta}{\lambda_+ - \lambda_-} \left[ \left( \frac{\gamma_{L\Gamma} + \lambda_+}{\lambda_+} \right) (e^{\lambda_+ t} - 1) \right. \\ &\quad \left. - \left( \frac{\gamma_{L\Gamma} + \lambda_-}{\lambda_-} \right) (e^{\lambda_- t} - 1) \right]. \end{aligned} \quad (16)$$

Some insight into the intervalley problem is obtained by looking at the limiting form for the eigenvalues in Eq. (11). As mentioned earlier, the detailed balance relation requires that  $\gamma_{\Gamma L}$  and  $\gamma_{L\Gamma}$  be in the ratio of the equilibrium populations  $R$ . Taking into account nonparabolicity of the  $\Gamma$  valley and the fourfold degeneracy of the  $L$  valleys,<sup>16</sup> for 2-eV photoexcitation in GaAs, electrons are photoexcited 0.5 eV above the bottom of the conduction band<sup>17,18</sup> and

$$R \equiv \frac{\gamma_{L\Gamma}}{\gamma_{\Gamma L}} = \frac{n_{\Gamma}^{\text{eq}}}{n_L^{\text{eq}}} \approx 0.1. \quad (17)$$

This ratio is large because the effective mass in the  $L$  valley is substantially greater than the effective mass in the  $\Gamma$  valley.<sup>19</sup> We also note that *nonparabolicity* is an important consideration in determining this ratio since at 0.5 eV nonparabolicity increases the density of states by 60% in the  $\Gamma$  valley.<sup>20</sup>

Because of the large value of  $R$ , it follows that  $\gamma_{L\Gamma} \ll \gamma_{\Gamma L}$  and the square root in Eq. (11) can be expanded to yield

$$\lambda_+ \approx -(\gamma_{\Gamma L} + \gamma_{\Delta}), \quad \lambda_- \approx \frac{-\gamma_{L\Gamma}\gamma_{\Delta}}{\gamma_{\Gamma L} + \gamma_{\Delta}}. \quad (18)$$

Note that for nonzero rates  $|\lambda_+| \gg |\lambda_-|$ .

There are two interesting cases depending on how the  $\Gamma \rightarrow L$  intervalley scattering rate compares with the inelastic scattering rate in the  $\Gamma$  valley. In the limit that  $\gamma_{\Delta} \ll \gamma_{\Gamma L}$ , i.e.,  $\Gamma \rightarrow L$  intervalley scattering is faster than POP scattering within the  $\Gamma$  valley, then

$$\lambda_- \approx -\frac{\gamma_{L\Gamma}}{\gamma_{\Gamma L}}\gamma_{\Delta} = -\frac{n_{\Gamma}^{\text{eq}}}{n_L^{\text{eq}}}\gamma_{\Delta} = -R\gamma_{\Delta}. \quad (19)$$

In this case,  $\lambda_-$  does not measure the  $L \rightarrow \Gamma$  scattering rate, but instead measures the product of the inelastic scattering rate and the ratio of the equilibrium populations  $R$ . Even though  $\gamma_{\Delta}$  might be greater than  $\gamma_{L\Gamma}$ , the net return of electrons from the  $L$  valleys is determined by how fast electrons relax to lower-energy levels within the  $\Gamma$  valley, not on how fast they scatter from the  $L$  valley to  $\Gamma$  valley.

For  $\gamma_{\Delta} \gg \gamma_{\Gamma L}$ , i.e., POP scattering is faster than the  $\Gamma \rightarrow L$  rate, we obtain

$$\lambda_- \approx -\gamma_{L\Gamma}. \quad (20)$$

This is, if electrons in the  $\Gamma$  valley are rapidly scattered to low-energy states, then the return time of the  $L$ -valley electrons is limited by the  $L \rightarrow \Gamma$  scattering rate. Only in this limit does the  $L$ -valley depopulation rate measure the  $L \rightarrow \Gamma$  scattering rate.

It is interesting to note that, although the scattering rates given by the  $\gamma$ 's in this model are constants, the densities given in Eq. (16) are not characterized by a single exponential decay. Therefore the depopulation rate of a given state [given by  $-d \ln(n)/dt$ ] is time dependent in spite of the fact that the scattering rates are constant. Furthermore, depending on the values for the scattering rates, the two eigenvalues  $\lambda_+$  and  $\lambda_-$  can differ by more than an order of magnitude, which leads to depopulation rates that can change rapidly on a short time scale. Thus the total number of scattering events from the  $\Gamma$  to  $L$  valley, which is proportional to  $n_{\Gamma>}(t)\gamma_{\Gamma L}$ , changes rapidly with time after the initial photoexcitation in agreement with earlier Monte Carlo calculations.<sup>21,22</sup> This change, however, reflects the time dependence of  $n_{\Gamma>}(t)$  and not the scattering rate  $\gamma_{\Gamma L}$ .

The three-state model can be applied to a large number of experiments that are sensitive primarily to which valley the electron populates. An example of such an experiment is that of Nuss, Auston, and Capasso (NAC).<sup>5</sup> In the NAC experiment,<sup>5</sup> the time-dependent reflectivity was measured on a femtosecond scale to infer the electron mobility as a function of time. Since the mobility of electrons in the  $\Gamma$  valley is nearly independent of energy, and the mobility of electrons in the  $L$  valleys is negligible by comparison,<sup>19</sup> a measure of the mobility as a function of time is a measure of the density of electrons in the  $\Gamma$  valley (without regard to which state within the  $\Gamma$  valley the electrons occupy). In the three-state model, the mobility is therefore proportional to

$$\frac{\mu(t)}{\mu(t \rightarrow \infty)} = \frac{n_{\Gamma>}(t) + n_{\Gamma<}(t)}{n_{\Gamma>}^0}. \quad (21)$$

To compare our calculations to the experiment, we must estimate the scattering rates. Based on the scattering rates of Schichijo and co-workers,<sup>23,24</sup> we estimate the rates to be given by

$$\begin{aligned} \gamma_{\Gamma L} &= 2 \times 10^{13} \text{ s}^{-1}, \\ R &\equiv \frac{\gamma_{L\Gamma}}{\gamma_{\Gamma L}} = 0.1, \\ \gamma_{\Delta} &= 5 \times 10^{12} \text{ s}^{-1}. \end{aligned} \quad (22)$$

In a later section, we show the sensitivity of the results to these values. The results of the three-state calculation are plotted in Figs. 3–6.

In Fig. 3, the experimental mobility from the NAC experiment<sup>5</sup> is shown as the solid line. The calculated

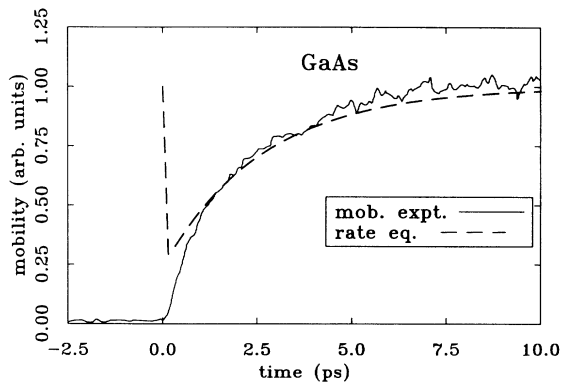


FIG. 3. The mobility vs time for GaAs as calculated from the three-state model. The solid line is the experimental work of Nuss, Auston, and Capasso (Ref. 5), the dashed line is the result from the three-state model. It is assumed that the mobility of electrons in the  $L$  valleys is close to zero while the mobility of the electrons in the  $\Gamma$  valley is independent of energy. The mobility is therefore proportional to the number of electrons in the  $\Gamma$  valley [ $n_{\Gamma>}(t) + n_{\Gamma<}(t)$ ]. The initial peak in the rate equation solution near  $t=0$  results from electrons initially photoexcited in the  $\Gamma$  valley that rapidly transfer into the  $L$  valley. This occurs on an extremely fast time scale and is not resolvable in the experimental data.

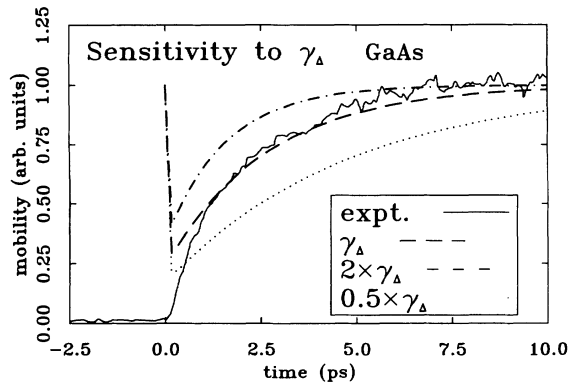


FIG. 4. Sensitivity of the rise time of the mobility to the inelastic (POP) scattering rate  $\gamma_{\Delta}$ . The solid line is the experimental data (Ref. 5), the dashed line the results of the three-state rate-equation model. For the dash-dotted line, the rate is doubled, whereas for the dotted line, the rate is cut in half. As can be seen, the rise time of the mobility is very sensitive to this quantity.

curve from the three-state model, Eq. (21), is shown as the dotted line. The two are in close agreement a short time after  $t=0$ . The peak in the rate equation model near  $t=0$  is caused by electrons initially excited in the  $\Gamma$  valley that quickly scatter to the  $L$  valleys. This fast initial transient is not resolvable in the experimental data and indicates that the initial  $\Gamma \rightarrow L$  transfer is rapid.

To test the sensitivity of the rate equation model, we vary the parameters. In Fig. 4, we show the sensitivity of the rise time of the mobility to the POP scattering rate  $\gamma_{\Delta}$ . The solid line corresponds to the experimental data

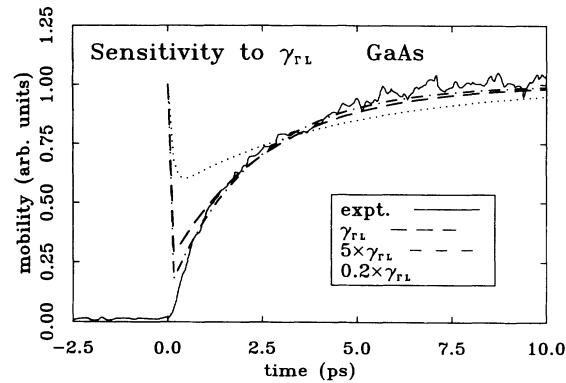


FIG. 5. Sensitivity of the rise time of the mobility to the intervalley scattering time  $\gamma_{\Gamma L}$ . The solid line is the experimental data (Ref. 5) and the dashed line the calculation. For the dash-dotted line, the intervalley rate  $\gamma_{\Gamma L}$  is increased by a factor of 5 as well as the  $L$  to  $\Gamma$  rate  $\gamma_{L\Gamma}$ , thus keeping the ratio  $R$  constant. As can be seen a fivefold increase does not significantly influence the results indicating the general insensitivity of the rise time to the intervalley scattering. When the rates are divided by a factor of 5, the dotted line results. When divided by a factor of 5, the intervalley scattering rate is slower than the POP rate and thus shows some discrepancy with the experiment at short times.

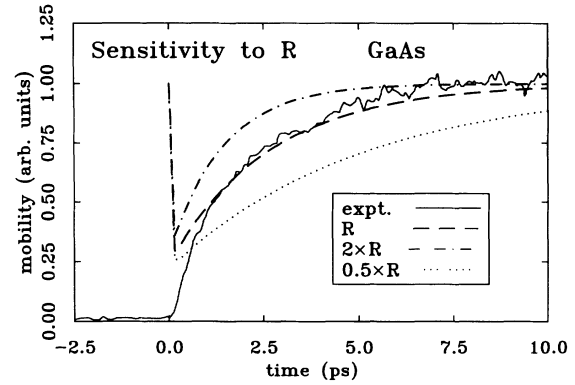


FIG. 6. Sensitivity of the rise time of the mobility to the equilibrium population ratio  $R$ . For the dash-dotted line, the  $L$  to  $\Gamma$  rate  $\gamma_{L\Gamma}$  is doubled keeping  $\gamma_{\Gamma L}$  constant and thus doubling the equilibrium population ratio  $R$ . For the dotted line, the ratio  $R$  is halved. As can be seen, the rise time of the mobility is very sensitive to this ratio.

of NAC, and the dashed line to the previous fit based on the rate-equation model (cf. Fig. 3). For the dash-dotted line, the POP rate is doubled, whereas for the dotted line, the POP rate is cut in half. As can be seen, the mobility and hence the number of electrons in the  $\Gamma$  valley depends strongly on the POP scattering rate. If the POP scattering rate is low,  $\gamma_{\Delta} \ll \gamma_{\Gamma L}$ , then according to Eq. (19), it takes longer to get a net transfer of electrons back into the (high mobility)  $\Gamma$  valley.

In Fig. 5, we show the sensitivity of the rise time of the mobility to the intervalley scattering rates. To do this, since we have shown that the  $L \rightarrow \Gamma$  and  $\Gamma \rightarrow L$  rates are dependent [cf. Eq. (7)], we vary both  $\gamma_{\Gamma L}$  and  $\gamma_{L\Gamma}$  but keep the ratio  $R$  constant. The solid line corresponds to the experimental data<sup>5</sup> and the dashed line the original fit. For the dash-dotted line,  $\gamma_{\Gamma L}$  and  $\gamma_{L\Gamma}$  are increased by a factor of 5, whereas for the dotted line, they are decreased by a factor of 5. As can be seen, the rise time is not strongly affected when the rate is increased, again consistent with Eq. (19), provided the ratio remains constant. When the rate is divided by a factor of 5, however, then one is no longer in the limit  $\gamma_{\Gamma L} \gg \gamma_{\Delta}$  and a slight change in the time-dependent mobility is observed at short times. For slow intervalley scattering, i.e.,  $0.2 \times \gamma_{\Gamma L}$ , there is not a rapid transfer of the initial electron populations into the  $L$  valleys as in the other cases. If the  $\Gamma \rightarrow L$  intervalley rate were this slow, one should see these effects in the experimental data. The fact that they are not seen shows that the  $\Gamma \rightarrow L$  rate cannot be this slow and indicates that the intervalley rate  $\gamma_{\Gamma L}$  is greater than the POP scattering rate  $\gamma_{\Delta}$ .

In Fig. 6, we show the sensitivity of the rise time of the mobility to the density of states ratio  $R$ . The solid line is the experimental data and the dashed line is from the original calculated results. In all cases, we hold  $\gamma_{\Gamma L}$  constant and vary  $\gamma_{L\Gamma}$  to change the ratio  $R$ . For the dash-dotted line, the ratio is doubled, whereas for the dotted line it is halved. We can see that the data are very sensi-

tive to this ratio. In fact, the curves are similar to those in Fig. 4, which we should expect based on Eq. (19).

These results show that the  $\Gamma \rightarrow L$  intervalley rate is faster than the POP rate. This agrees with the transient nonlinear absorption experiments of Rosker, Wise, and Tang,<sup>7</sup> Schoenlein *et al.*,<sup>8</sup> and Becker *et al.*,<sup>9,10</sup> which predict fast  $\Gamma \rightarrow L$  rates. Also, even though the  $L \rightarrow \Gamma$  rate is slower than the POP rate, the return time of carriers from the  $L$  valley is still limited by the relaxation of the electrons in the  $\Gamma$  valley.

#### FOUR-STATE MODEL

The three-state model is useful for determining the  $\Gamma$ - and  $L$ -valley populations and is applicable for describing experiments which depend only on which valley the electrons occupy. Other experiments, such as the rise time of the band-edge photoluminescence, are more sensitive to the *state within the  $\Gamma$  valley* that the electrons occupy. In particular, the photoluminescence experiments require that the electrons be at the bottom of the conduction band to contribute. Therefore the three-state model is not applicable. To account for this additional structure, we propose the four-state model shown schematically in Fig. 7. In the four-state model, an additional state is added in the  $\Gamma$  valley representing electrons at the band edge and is labeled  $\Gamma_{BE}$ . The  $\Gamma^<$  state now represents all the electrons with energies ranging from one optic phonon energy above the band edge to energies just below the threshold for scattering to the  $L$  valley. For an electron to scatter from the top of the  $\Gamma^<$  state to the bottom of the  $\Gamma$  valley into the  $\Gamma_{BE}$  state, requires that the electron emit approximately eight optical phonons (the first seven emissions keep the electron within the  $\Gamma^<$  state). The scattering rate from  $\Gamma^<$  to  $\Gamma_{BE}$ , denoted by  $\gamma_{BE}$ , is therefore approximately  $\gamma_{\Delta}/8$ .

In matrix form, the four-state model is given as

$$\frac{d}{dt} \begin{pmatrix} n_{\Gamma^>} \\ n_L \\ n_{\Gamma^<} \\ n_{\Gamma_{BE}} \end{pmatrix} = \begin{pmatrix} -(\gamma_{\Gamma L} + \gamma_{\Delta}) & \gamma_{L\Gamma} & 0 & 0 \\ \gamma_{\Gamma L} & -\gamma_{L\Gamma} & 0 & 0 \\ \gamma_{\Delta} & 0 & -\gamma_{BE} & 0 \\ 0 & 0 & \gamma_{BE} & 0 \end{pmatrix} \times \begin{pmatrix} n_{\Gamma^>} \\ n_L \\ n_{\Gamma^<} \\ n_{\Gamma_{BE}} \end{pmatrix}. \quad (23)$$

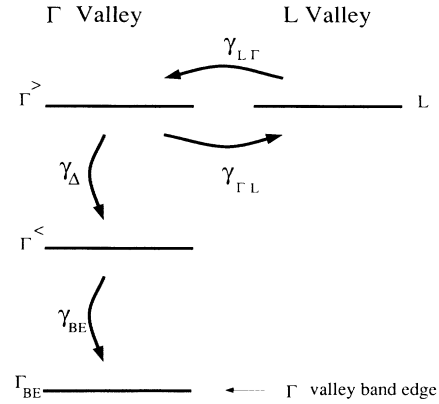


FIG. 7. The four-state model. Here  $\Gamma^>$  represents electrons in the  $\Gamma$  valley that are energetically able to transfer to the  $L$ -valley state.  $\Gamma^<$  includes all electrons in the  $\Gamma$  valley that are just below the energy threshold for transfer to the  $L$  valley to those electrons that are just above the band edge.  $\Gamma_{BE}$  represents the electrons in the  $\Gamma$  valley at the band edge. Band-edge photoluminescence is sensitive to the number of electrons in the  $\Gamma_{BE}$  state. Scattering from  $\Gamma^<$  to  $\Gamma_{BE}$  involves the emission of several phonons (approximately 8 in GaAs) for electrons to go from just below the threshold for intervalley transfer to the bottom of the band edge, and the rate is given by  $\gamma_{BE}$ .

The eigenvalues for this matrix are easily found by expanding the determinant by cofactors of the last column. They are 0,  $\lambda_+$ ,  $\lambda_-$ , and  $-\gamma_{BE}$ .

One can solve Eq. (23) by noting that the coupled equations for  $n_{\Gamma^>}$  and  $n_L$  are the same as before, and that the expression for  $n_{\Gamma^<}$  can be found by using an integrating factor and directly integrating the previous expressions. The expression for  $n_{BE}$  can then be found by integrating the expression for  $n_{\Gamma^<}$ ,

$$n_{\Gamma^<}(t) = \gamma_{\Delta} \int_0^t dt' e^{-\gamma_{BE}(t-t')} n_{\Gamma^>}(t'), \quad (24)$$

$$n_{\Gamma_{BE}}(t) = \gamma_{BE} \int_0^t dt' n_{\Gamma^<}(t').$$

From these equations, one obtains the solutions

$$n_{\Gamma^<}(t) = \frac{n_{\Gamma^>}^0 \gamma_{\Delta}}{\lambda_+ - \lambda_-} \left[ \left( \frac{\gamma_{L\Gamma} + \lambda_+}{\lambda_+ + \gamma_{BE}} \right) (e^{\lambda_+ t} - e^{-\gamma_{BE} t}) - \left( \frac{\gamma_{L\Gamma} + \lambda_-}{\lambda_- + \gamma_{BE}} \right) (e^{\lambda_- t} - e^{-\gamma_{BE} t}) \right], \quad (25)$$

$$n_{\Gamma_{BE}}(t) = \frac{n_{\Gamma^>}^0 \gamma_{\Delta} \gamma_{BE}}{\lambda_+ - \lambda_-} \left[ \left( \frac{\gamma_{L\Gamma} + \lambda_+}{\lambda_+ + \gamma_{BE}} \right) \left[ \frac{(e^{\lambda_+ t} - 1)}{\lambda_+} + \frac{(e^{-\gamma_{BE} t} - 1)}{\gamma_{BE}} \right] - \left( \frac{\gamma_{L\Gamma} + \lambda_-}{\lambda_- + \gamma_{BE}} \right) \left[ \frac{(e^{\lambda_- t} - 1)}{\lambda_-} + \frac{(e^{-\gamma_{BE} t} - 1)}{\gamma_{BE}} \right] \right]. \quad (26)$$

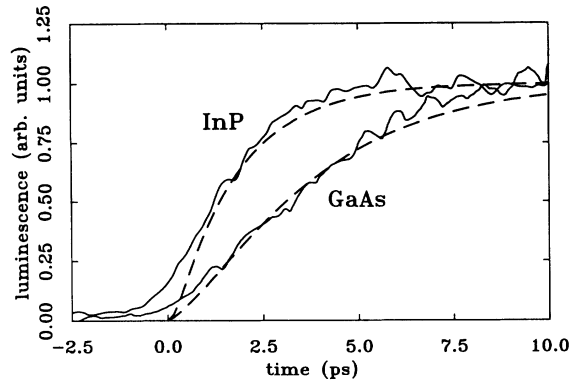


FIG. 8. Rise time for the luminescence in GaAs and InP as calculated from the four-state model. The solid lines are from the experimental work of Shah *et al.* (Ref. 2). The dashed lines are the results of the four-state model. For InP, the intervalley scattering rates  $\gamma_{\Gamma L}$  and  $\gamma_{L\Gamma}$  are set to zero keeping all other rates the same. As can be seen, the rate-equation model accurately predicts the observed differences between GaAs and InP. Differences between the experimental curves and rate-equation model at short times originate from the finite temporal width of the laser pulse not accounted for in the four-state model.

Results for the four-state model are shown in Figs. 8–12. The experimental luminescence is proportional to the density of electrons at the bottom of the band, i.e., the population of  $\Gamma_{BE}$ . In Fig. 8, we show the experimental data for the rise time of the luminescence in GaAs and InP from Shah *et al.*<sup>2</sup> (solid lines). We also plot the results of the four-state model (dashed lines). We use a  $\gamma_{BE}$  rate of  $6 \times 10^{11} \text{ s}^{-1}$ , approximately  $\frac{1}{8}$  of  $\gamma_{\Delta}$ . For InP, since the  $L$  valleys lie too high in energy for intervalley transfer in the Shah *et al.* experiment,<sup>2</sup> we set the intervalley rates to zero keeping all other rates the same. As can be seen from the curves, the rate-equation model ac-

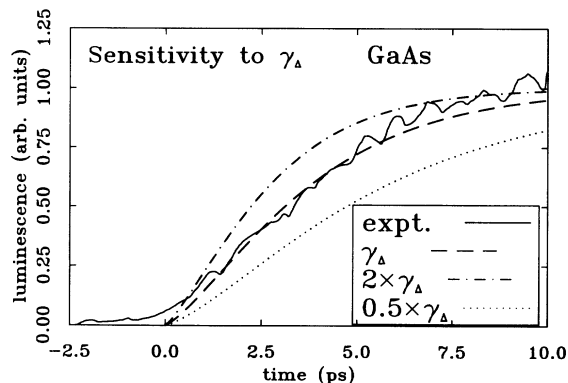


FIG. 9. Sensitivity of the rise time of the luminescence for GaAs in the four-state model to the electron-phonon scattering rate ( $\gamma_{\Delta}$ ). The solid line is the experimental data of Shah *et al.* (Ref. 2) and the dashed line is the result of the four-state model. For the dash-dotted line, the electron-phonon scattering rate is doubled, while for the dotted line, the rate is halved. As can be seen, the rise time of the luminescence is very sensitive to this rate.

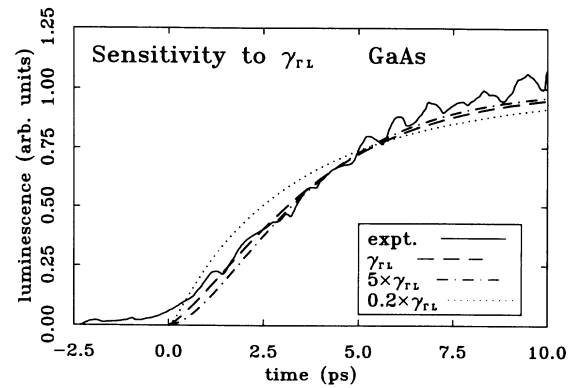


FIG. 10. Sensitivity of the rise time of the luminescence in GaAs to the intervalley scattering rate. The solid line is the experimental curve of Shah *et al.* (Ref. 2), and the dashed line the result of the four-state model. For the dash-dotted and dotted lines, the intervalley scattering rates are changed so that the ratio  $R$  remains constant. For the dash-dotted line the rate is increased by a factor of 5, while for the dotted line, the rate is divided by a factor of 5. As can be seen from the figures, the rise time of the luminescence is *insensitive* to the intervalley rates provided the ratio of the equilibrium populations is constant.

curately predicts the dependence of the rise time of the luminescence for both InP and GaAs. Since the total number of electrons in the  $\Gamma$  valley as a function of time does not change between the three-state and four-state models (only the occupation of the different  $\Gamma$  valley states changes), the rise time of the mobility is exactly the same as before.

In Fig. 9, we check the sensitivity of the luminescence rise time to the POP scattering rate. The solid line is from the experiment,<sup>2</sup> the dashed is from the original fit, and the dash-dotted and dotted correspond to doubling and halving the POP rate, respectively. Just as for the

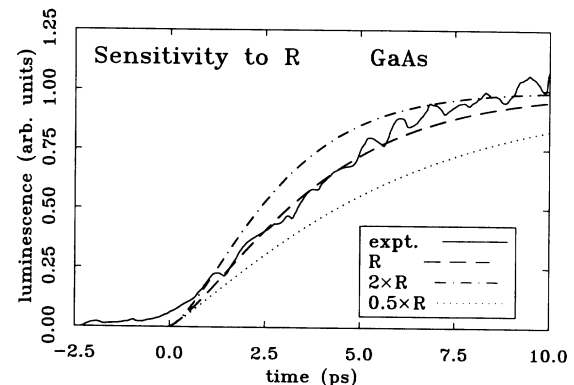


FIG. 11. Sensitivity of the rise time of the luminescence in GaAs to the density of state ratio  $R$ . The solid line is the experimental work of Shah *et al.* (Ref. 2) and the dashed line the solution to the four-state model. For the dash-dotted line, the ratio of the populations is doubled, while for the dotted line, it is cut in half. The curves are similar to those in Fig. 9, showing that the rise time of the luminescence depends on the rate  $\gamma_{\Delta}$  (as well as  $\gamma_{BE}$ ).

mobility, we see that the rise time of the luminescence is very sensitive to this rate. The net transfer of carriers from the  $L$  to the  $\Gamma$  valley depends strongly on the POP scattering rate within the  $\Gamma$  valley.

In Fig. 10, we show the sensitivity of the luminescence to the intervalley scattering rates keeping the ratio  $R$  constant. As before, there is not a strong dependence on the magnitude of the rate, even when divided by a factor of 5, provided the ratio is kept constant. We thus see that experiments measuring the rise time of the luminescence are insensitive to the intervalley rates, and only depend on the density of states in the two valleys and the inelastic scattering rate within the  $\Gamma$  valley.

In Fig. 11, we show the sensitivity to the ratio  $R$ . Again, the luminescence is sensitive to this ratio as predicted by Eq. (19).

### CONCLUSIONS

We have provided and solved a set of rate equations for intervalley scattering in compound semiconductors such as GaAs or InP. Using standard values for the transport parameters, solutions to these rate-equation models predict the experimental trends in time-dependent mobility and luminescence experiments quite well. Although these rate equations are simpler than full Monte Carlo modeling<sup>17,18</sup> or numerical solutions to the Boltzmann equation,<sup>25</sup> they nonetheless illustrate several key points.

(i) The  $\Gamma \rightarrow L$  and the  $L \rightarrow \Gamma$  intervalley scattering rates are *dependent* and related, through detailed balance, to the densities of states in each valley.

(ii) In time-dependent mobility and time-resolved photoluminescence experiments, one measures the *depopulation rate* of the  $L$  valley. The depopulation rate of the  $L$  valleys is *not* the same as the  $L \rightarrow \Gamma$  intervalley scattering rate unless the inelastic-scattering rate in the  $\Gamma$  valley is significantly larger than the  $\Gamma \rightarrow L$  rate. From an estimate of the transport parameters that are applicable to GaAs and InP, we find excellent agreement between the

rate equations and experimental data for both the time-dependent mobility and the rise time of the luminescence. The scattering rates suggest that the  $L$ -valley depopulation is dominated by the energy relaxation of the electrons in the  $\Gamma$  valley. That is, POP scattering in the  $\Gamma$  valley acts as the bottleneck for the return of the electrons from the  $L$  valley. This return is not limited by the  $L \rightarrow \Gamma$  intervalley scattering rate. This suggests that time dependent mobility and band-edge luminescence experiments are not optimum for determining the intervalley scattering rates.

(iii) The initial low mobility in the NAC experiment can only be explained by a rapid transfer of electrons from their photoexcited states into the  $L$  valleys, suggesting a fast  $\Gamma \rightarrow L$  rate. This is consistent with the insensitivity of the rise time of the luminescence in GaAs to the  $\Gamma \rightarrow L$  rate, as well as the transient nonlinear absorption experiments of Rosker, Wise, and Tang,<sup>7</sup> Schoenlein *et al.*,<sup>8</sup> and Becker *et al.*,<sup>9,10</sup> which predict fast  $\Gamma \rightarrow L$  rates. Thus this is further evidence that the  $\Gamma \rightarrow L$  intervalley scattering rate is *faster* than the POP scattering rate.

While the rate equation models are simple, they nonetheless provide valuable insight into the qualitative carrier dynamics in compound semiconductors and isolate characteristics often lost in more detailed calculations.

### ACKNOWLEDGMENTS

We are thankful to Frank Wise and Pradeep Kumar for useful discussions during this work. We are also grateful for the hospitality of the Institute for Theoretical Physics where part of this work was completed. This work was supported in part by the National Science Foundation through Grants Nos. DMR8957382 and PHY89-04035 and by the U.S. Office of Naval Research through Grant No. N00091-J-1956.

<sup>1</sup>S. M. Sze, *Physics of Semiconductor Devices*, 2nd ed. (Wiley, New York, 1981), Chap. 11.

<sup>2</sup>J. Shah, B. Deveaud, T. C. Damen, W. T. Tsang, A. C. Gosard, and P. Lugli, *Phys. Rev. Lett.* **59**, 222 (1987).

<sup>3</sup>T. Elsaesser, J. Shah, L. Rota, and P. Lugli, *Phys. Rev. Lett.* **66**, 1757 (1991).

<sup>4</sup>W. B. Wang, N. Ockman, M. A. Cavicchia, and R. R. Alfano, *Appl. Phys. Lett.* **57**, 395 (1990).

<sup>5</sup>M. C. Nuss, D. H. Auston, and F. Capasso, *Phys. Rev. Lett.* **58**, 2355 (1987).

<sup>6</sup>C. L. Tang, I. A. Walmsley, and F. W. Wise, *Appl. Phys. Lett.* **52**, 850 (1988).

<sup>7</sup>M. Rosker, F. Wise, and C. L. Tang, *Appl. Phys. Lett.* **49**, 1726 (1986).

<sup>8</sup>R. W. Schoenlein, W. Z. Lin, S. D. Brorson, E. P. Ippen, and J. G. Fujimoto, *Appl. Phys. Lett.* **51**, 1442 (1987).

<sup>9</sup>P. C. Becker, H. L. Fragnito, C. H. Brito Cruz, J. Shah, R. L. Fork, J. E. Cunningham, J. E. Henry, and C. V. Shank, *Appl.*

*Phys. Lett.* **53**, 2089 (1988).

<sup>10</sup>P. C. Becker, H. L. Fragnito, C. H. Brito Cruz, R. L. Fork, J. E. Cunningham, J. E. Henry, and C. V. Shank, *Phys. Rev. Lett.* **61**, 1647 (1988).

<sup>11</sup>B. P. Zakharchenya, D. N. Mirlin, V. I. Perel, and I. I. Reshina, *Usp. Fiz. Nauk.* **136**, 459 (1982) [*Sov. Phys. Usp.* **25**, 143 (1982)].

<sup>12</sup>G. Fasol, W. Hackenberg, H. P. Hughes, K. Ploog, E. Bauser, and H. Kano, *Phys. Rev. B* **41**, 1461 (1990).

<sup>13</sup>R. G. Ulbrich, J. A. Kash, and J. C. Tsang, *Phys. Rev. Lett.* **62**, 949 (1989).

<sup>14</sup>C. J. Stanton, Ph.D. thesis, Cornell University, 1986.

<sup>15</sup>K. Hess, *Advanced Theory of Semiconductor Devices* (Prentice-Hall, Englewood Cliffs, NJ, 1988).

<sup>16</sup>F. H. Pollak, C. W. Higginbotham, and M. Cardona, *J. Phys. Soc. Jpn. Suppl.* **21**, 20 (1966).

<sup>17</sup>C. J. Stanton, D. W. Bailey, and K. Hess, *Phys. Rev. Lett.* **65**, 231 (1990).

- <sup>18</sup>D. W. Bailey, C. J. Stanton, and K. Hess, *Phys. Rev. B* **42**, 3423 (1990).
- <sup>19</sup>E. M. Conwell, in *Solid State Physics, Advances in Research and Applications*, edited by F. Seitz, D. Turnbull, and H. Ehrenreich (Academic, New York, 1967), Vol. 9.
- <sup>20</sup>L. Reggiani, in *Hot-Electron Transport in Semiconductors*, edited by L. Reggiani (Springer-Verlag, Berlin, 1985), Chap. 2.
- <sup>21</sup>D. W. Bailey *et al.*, *Solid-State Electron.* **31**, 467 (1988).
- <sup>22</sup>M. J. Kann, A. M. Kriman, and D. K. Ferry, *Solid-State Electron.* **32**, 1831 (1989).
- <sup>23</sup>H. Shichijo and K. Hess, *Phys. Rev. B* **23**, 4197 (1981).
- <sup>24</sup>H. Shichijo, Ph.D. thesis, University of Illinois, 1980.
- <sup>25</sup>Y. S. Sun and C. J. Stanton, *Phys. Rev. B* **43**, 2285 (1991).